

Carbon–Oxygen Bond Cleavage with η^9, η^5 -Bis(indenyl)zirconium Sandwich Complexes

Christopher A. Bradley,[†] Luis F. Veiros,[‡] Doris Pun,[†] Emil Lobkovsky,[†]
Ivan Keresztes,[†] and Paul J. Chirik^{*,†}

Contribution from the Department of Chemistry and Chemical Biology, Baker Laboratory, Cornell University, Ithaca, New York 14853, and Centro de Química Estrutural, Complexo I, Instituto Superior Técnico, Av. Rovisco Pais 1, 1049-001 Lisbon, Portugal

Received July 28, 2006; E-mail: pc92@cornell.edu

Abstract: Treatment of the η^9, η^5 -bis(indenyl)zirconium sandwich complex, $(\eta^9\text{-C}_9\text{H}_5\text{-1,3-(SiMe}_3)_2)(\eta^5\text{-C}_9\text{H}_5\text{-1,3-(SiMe}_3)_2\text{Zr)}$, with dialkyl ethers such as diethyl ether, CH_3OR ($\text{R} = \text{Et, } ^t\text{Bu, } ^i\text{Bu}$), $^t\text{Bu}_2\text{O}$, or $^i\text{Pr}_2\text{O}$ resulted in facile C–O bond scission furnishing an η^5, η^5 -bis(indenyl)zirconium alkoxy hydride complex and free olefin. In cases where ethylene is formed, trapping by the zirconocene sandwich yields a rare example of a crystallographically characterized, base-free η^5, η^5 -bis(indenyl)zirconium ethylene complex. Observation of normal, primary kinetic isotope effects in combination with rate studies and the stability of various model compounds support a mechanism involving rate-determining C–H activation to yield an η^5, η^5 -bis(indenyl)zirconium alkyl hydride intermediate followed by rapid β -alkoxide elimination. For isolable η^6, η^5 -bis(indenyl)zirconium THF compounds, thermolysis at 85 °C also resulted in C–O bond cleavage to yield the corresponding zirconacycle. Both mechanistic and computational studies again support a pathway involving haptotropic rearrangement to η^5, η^5 -bis(indenyl)zirconium intermediates that promote rate-determining C–H activation and ultimately C–O bond scission.

Introduction

The rich chemistry of low oxidation state, reducing group 4 transition metal complexes continues to attract considerable attention given the utility of these compounds to promote numerous organic transformations¹ and small molecule activation processes.² Substituted bis(cyclopentadienyl) complexes of titanium and zirconium (group 4 metallocenes) have been the most extensively studied, owing to their commercial availability, steric and electronic modularity, and convenient synthetic access to low oxidation states by treatment with alkyl lithium reagents³ or alkali metal reductants.⁴

The first isolable examples⁵ of bis(cyclopentadienyl)titanium-(II) sandwiches were independently reported by Lawless⁶ and Mach.⁷ These compounds of the general form $(\eta^5\text{-C}_5\text{Me}_4\text{R})_2\text{Ti}$

are stabilized by the introduction of sterically demanding silyl substituents ($\text{R} = \text{SiMe}_3, \text{SiMe}_2^t\text{Bu}, \text{SiMe}_2\text{Ph}$, etc.) on the cyclopentadienyl rings. Subsequent studies from our laboratory have demonstrated that exposure of many of these compounds to dinitrogen at low temperature yields monomeric bent titanocene mono- and bis(dinitrogen) complexes, depending on the specific cyclopentadienyl substituent.⁸ This chemistry has recently been extended to the isolobal and isoelectronic carbon monoxide derivatives, $(\eta^5\text{-C}_5\text{Me}_4\text{R})_2\text{Ti}(\text{CO})$, and the observation of mixed titanocene dinitrogen, carbonyl compounds.⁹

Such an approach has not been successful for the preparation of the corresponding bis(cyclopentadienyl)zirconium(II) sandwich compounds.¹⁰ The larger metallic atomic radius and greater thermodynamic driving force to achieve the +4 oxidation state make such targets more challenging to access. Our laboratory has discovered that replacing the cyclopentadienyl anions with related six π -electron, 1,3-disubstituted indenyl ligands has allowed observation¹¹ and ultimately complete spectroscopic and structural characterization¹² of the first bis(indenyl)zirconium

[†] Cornell University.

[‡] Instituto Superior Técnico.

- (1) For a recent review, see: *Titanium and Zirconium in Organic Synthesis*; Marek, I., Ed.; Wiley-VCH: Weinheim, 2002.
- (2) (a) Pool, J. A.; Chirik, P. J. *Can. J. Chem.* **2005**, *83*, 286. (b) Fryzuk, M. D.; Johnson, S. A. *Coord. Chem. Rev.* **2000**, *200*, 379.
- (3) (a) Negishi, E.-I.; Takahashi, T. *Acc. Chem. Res.* **1994**, *27*, 124. (b) Rosenthal, U.; Pellny, P.-M.; Kirchner, F. G.; Burkalov, V. V. *Acc. Chem. Res.* **2000**, *33*, 119.
- (4) (a) Gambarotta, S.; Scott, J. *Angew. Chem., Int. Ed.* **2004**, *43*, 5298. (b) Fryzuk, M. D. *Chem. Rec.* **2003**, *3*, 2.
- (5) For observation of bis(cyclopentadienyl)titanium sandwich complexes in solution see: (a) Bercaw, J. E.; Brintzinger, H. H. *J. Am. Chem. Soc.* **1971**, *93*, 2045. (b) Bercaw, J. E. *J. Am. Chem. Soc.* **1974**, *96*, 5087. (c) deWolf, J. M.; Blaauw, R.; Meetsma, A.; Teuben, J. H.; Gyepes, R.; Varga, V.; Mach, K.; Veldman, N.; Spek, A. L. *Organometallics* **1996**, *15*, 4977. (d) Hanna, T. E.; Keresztes, I.; Lobkovsky, E.; Bernskoetter, W. H.; Chirik, P. J. *Organometallics* **2004**, *23*, 3448.
- (6) Hitchcock, P. B.; Kerton, F.; Lawless, G. A. *J. Am. Chem. Soc.* **1998**, *120*, 10264.

- (7) Lukesová, L.; Horáček, M.; Stepnicka, P.; Fejfarová, K.; Gyepes, R.; Cisorová, I.; Kubista, J.; Mach, K. *J. Organomet. Chem.* **2002**, *663*, 134.
- (8) Hanna, T. E.; Lobkovsky, E.; Chirik, P. J. *J. Am. Chem. Soc.* **2004**, *126*, 14688.
- (9) Hanna, T. E.; Lobkovsky, E.; Chirik, P. J. *J. Am. Chem. Soc.* **2006**, *128*, 6018.
- (10) Horáček, M.; Stepnicka, P.; Kubista, J.; Fejfarová, K.; Gyepes, R.; Mach, K. *Organometallics* **2003**, *22*, 861.
- (11) Bradley, C. A.; Lobkovsky, E.; Chirik, P. J. *J. Am. Chem. Soc.* **2003**, *125*, 8110.
- (12) Bradley, C. A.; Keresztes, I.; Lobkovsky, E.; Young, V. G.; Chirik, P. J. *J. Am. Chem. Soc.* **2004**, *126*, 16937.

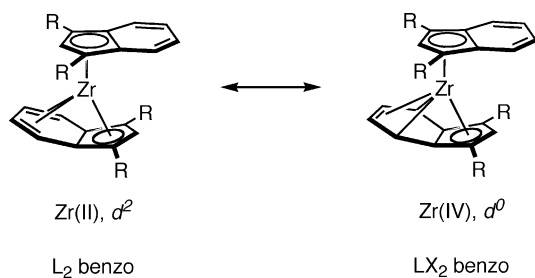
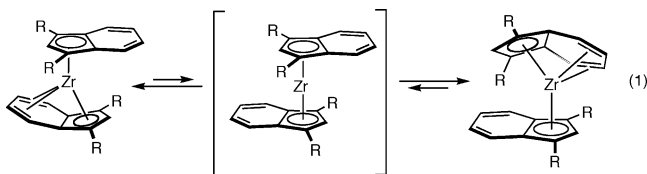


Figure 1. Bonding description for η^9, η^5 -bis(indenyl)zirconium sandwich compounds.

sandwich complexes. As was computationally predicted,¹³ these compounds do not adopt the familiar parallel ring structure typically associated with bis(cyclopentadienyl)metal sandwich complexes but rather contain one “ η^9 ” indenyl ring where the carbocycle is buckled and all nine carbons of the ligand are coordinated to the zirconium.¹⁴ A more detailed investigation into the electronic structure of these compounds¹³ has established a bonding description between two limiting canonical forms. In one extreme, the η^9, η^5 -bis(indenyl)zirconium sandwich can be viewed as a Zr(II), d^2 species with a neutral benzo ligand while in the other as a Zr(IV), d^0 complex where the benzo ring is reduced by two electrons to form an LX_2 fragment (Figure 1).

In light of these results, the possibility for these molecules to serve as sources of $[\eta^5-(C_9H_5-1,3-R_2)_2Zr^{II}]^{15}$ by dissociation of the benzo portion of the η^9 indenyl ring has been an area of considerable experimental and theoretical interest. Both line broadening and EXSY NMR experiments have established that the η^9, η^5 -bis(indenyl)zirconium sandwich complexes undergo facile ($\Delta G_{296}^\ddagger \approx 14$ – 20 kcal/mol) ring interchange in solution, most likely involving the desired $[\eta^5-(C_9H_5-1,3-R_2)_2Zr^{II}]$ intermediate (eq 1).¹² These experiments have been supported by



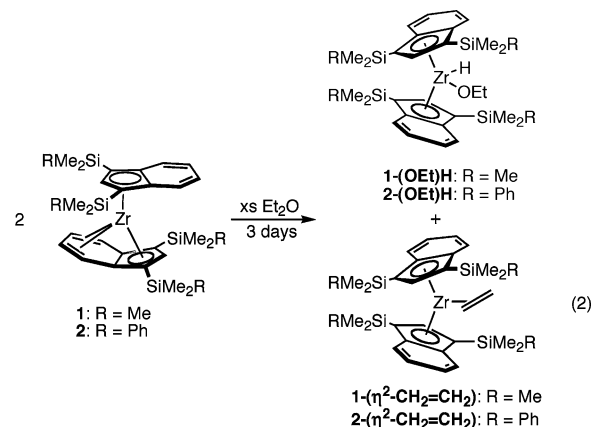
computational studies, where a dissociative mechanism generating an $[\eta^5-(C_9H_5-1,3-R_2)_2Zr^{II}]$ ($S = 0$) species was found to be the lowest energy pathway.¹⁶

In this contribution, the reactivity of η^9, η^5 -bis(indenyl)zirconium sandwich complexes toward dialkyl ethers and THF is explored both experimentally and computationally. Carbon–oxygen bond cleavage has been observed under mild conditions in solution and was found to proceed through reducing η^9, η^5 -bis(indenyl)zirconium intermediates that promote initial C–H activation followed by C–O bond scission.

Results and Discussion

Carbon–Oxygen Bond Cleavage in Dialkyl Ethers. Interest in the reactivity of η^9, η^5 -bis(indenyl)zirconium sandwich compounds with dialkyl ethers stems from the observation of ligand-induced η^9 to η^6 haptotropic rearrangement upon addition of THF or DME (DME = 1,2-dimethoxyethane).¹⁷ Computational studies suggest that migration of the metal to the benzo rather than cyclopentadienyl ring allows additional backbonding with the six-membered ring thereby stabilizing the η^6 over the η^5 haptomer.¹⁸ In this study, the scope of this transformation was explored with simple, commercially available dialkyl ethers.

Stirring either of the silyl-substituted η^9, η^5 -bis(indenyl)zirconium sandwich complexes, **1** or **2**, in diethyl ether at 23 °C resulted in cleavage of the C–O bond to form an equimolar mixture of the zirconocene ethoxy hydrides, (η^5 - C_9H_5 -1,3-($SiMe_2R$)₂)₂Zr(OCH₂CH₃)H (R = Me, **1-(OEt)H**; R = Ph, **2-(OEt)H**), and the corresponding ethylene compounds, (η^5 - C_9H_5 -1,3-($SiMe_2R$)₂)₂Zr(η^2 -CH₂=CH₂) (R = Me, **1-(η^2 -CH₂=CH₂)**; R = Ph, **2-(η^2 -CH₂=CH₂)**) (eq 2).



For diethyl ether cleavage with **1**, recrystallization of the product mixture from pentane at -35 °C furnished crystals of pure **1-(η^2 -CH₂=CH₂)**. Attempts to isolate the remaining **1-(OEt)H** from the mother liquor have been unsuccessful due to cocrystallization with **1-(η^2 -CH₂=CH₂)**. The identity of the zirconocene ethylene compound was further established by independent synthesis, as treatment of **1** with 1 equiv of CH₂=CH₂ also afforded **1-(η^2 -CH₂=CH₂)**. The ¹H and ¹³C NMR spectra of **1-(η^2 -CH₂=CH₂)** exhibit the number of peaks for a C_{2v} symmetric bent zirconocene derivative with two equivalent η^5, η^5 -coordinated indenyl rings. One notable feature of the benzene-*d*₆ ¹H NMR spectrum of **1-(η^2 -CH₂=CH₂)** is the observation of a broad singlet centered at 0.87 ppm for the vinylic hydrogens of the coordinated olefin. Confirmation of this assignment was provided by the preparation of **1-(η^2 -CD₂=CD₂)** from the cleavage of diethyl ether-*d*₁₀ or by treatment of **1** with CD₂=CD₂.

Single crystals of **1-(η^2 -CH₂=CH₂)** were obtained from a concentrated pentane solution chilled to -35 °C. Two independent, nearly identical molecules were found in the asymmetric unit, one of which is shown in Figure 2. Selected metrical parameters are reported in Table 1. Consistent with the solution NMR data, the indenyl rings are η^5 coordinated with a rotational

(13) Veiros, L. F. *Chem.–Eur. J.* **2005**, *11*, 2505.

(14) For a review on indenyl hapticity, see: Calhorda, M. J.; Romão, C. C.; Veiros, L. F. *Chem.–Eur. J.* **2002**, *8*, 868.

(15) For recent examples of accessing low-valent early transition metals by dissociation of a ligand, see: (a) Korobkov, I.; Arunachalampillai, A.; Gambarotta, S. *Organometallics* **2004**, *23*, 6248. (b) Korobkov, I.; Gambarotta, S.; Yap, G. P. A. *Angew. Chem., Int. Ed.* **2003**, *42*, 814. (c) Evans, W. J.; Davis, B. L. *Chem. Rev.* **2002**, *102*, 2119. (d) Diaconescu, P.; Arnold, P. L.; Baker, T.; Mendiola, D. J.; Cummins, C. C. *J. Am. Chem. Soc.* **2000**, *122*, 6108. (e) Tsai, Y.-C.; Johnson, M. A.; Mendiola, D. J.; Cummins, C. C.; Klooster, W. T.; Koetzle, T. F. *J. Am. Chem. Soc.* **1999**, *121*, 10426.

(16) Veiros, L. F. *Organometallics* **2006**, *25*, 2266.

(17) Bradley, C. A.; Kerestzes, I.; Lobkovsky, E.; Chirik, P. J. *J. Am. Chem. Soc.* **2005**, *127*, 10291.

(18) Veiros, L. F. *Organometallics* **2006**, *25*, 4698.

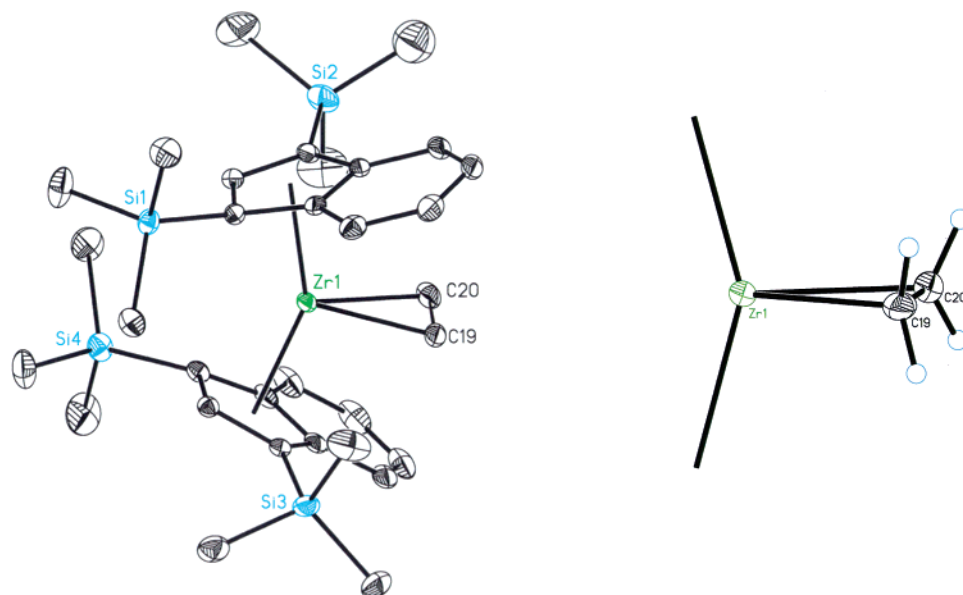


Figure 2. Molecular structure of **1**-(η^2 -CH₂=CH₂) (left) at 30% probability ellipsoids. Hydrogen atoms omitted for clarity. View of the core of the molecule (right).

Table 1. Selected Bond Distances (Å) and Angles (deg) for **1**-(η^2 -CH₂=CH₂)

C(19)–C(20)	1.443(5)
Zr(1)–C(19)	2.285(3)
Zr(1)–C(20)	2.278(3)
α^a	63(3)
slip distortions ^b	0.100(2), 0.1176(3)
fold angles	3.2(4), 3.3(2)
rotational angle	116.8(3)

^a Angle defined by the normals of the C–H–H planes. ^b For definitions of these parameters, see ref 24.

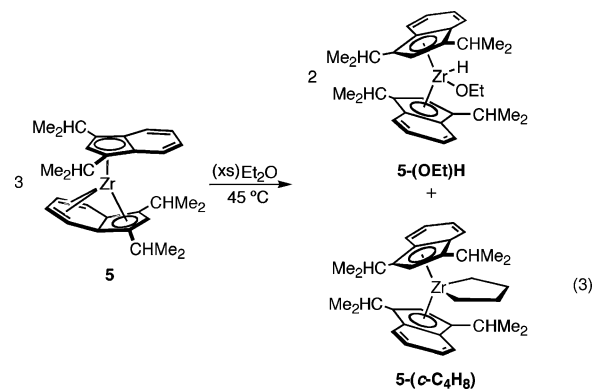
angle of 116.8(3)°. As expected for a bent zirconocene derivative, the ethylene ligand lies in the plane of the metallocene wedge with a C(19)–(20) bond distance of 1.443(5) Å and an α value of 63(3)°, consistent with the significant contribution from the zirconacyclopropane descriptor. This view is also corroborated by the ¹H NMR chemical shift, where the vinylic protons of the coordinated olefin are substantially shifted upfield from the typical alkene region of the spectrum.

While implicated as intermediates in zirconocene-promoted coupling reactions, isolable and crystallographically characterized base-free olefin complexes of group 4 metallocenes are rare.¹⁹ Despite the absence of a supporting ligand, the carbon–carbon bond distance in **1**-(η^2 -CH₂=CH₂) is statistically indistinguishable from the values of 1.451(5) and 1.455(9) Å reported for the base-stabilized complexes, (η^5 -C₉H₇)₂Zr(η^2 -CH₂=CH₂)(THF) and (η^5 -C₅H₅)₂Zr(η^2 -CH₂=CH₂)(THF), respectively.²⁰ These values are also in agreement with an *ansa*-zirconocene ethylene hydride anion²¹ as well as the permethyltitanocene ethylene complex, (η^5 -C₅Me₅)₂Ti(η^2 -CH₂=CH₂).²²

Characterization of the diethyl ether cleavage products from **2** was also accomplished by NMR spectroscopy, combustion

analysis, and degradation experiments. Similar to **1**-(η^2 -CH₂=CH₂), **2**-(η^2 -CH₂=CH₂) exhibited a singlet centered at 0.53 ppm for the vinylic hydrogens of the coordinated ethylene, consistent with zirconacyclopropane character. On a preparative scale, recrystallization of the product mixture from pentane at –35 °C yielded pure **2**-(OEt)H, opposite of the purification product isolated from **1**. Attempts to isolate pure **2**-(η^2 -CH₂=CH₂) have been unsuccessful due to contamination from **2**-(OEt)H. For both **1** and **2**, attempts were made to detect an intermediate η^6, η^5 -bis(indenyl)zirconocene diethyl ether complex by ¹H NMR spectroscopy. However, addition of a large excess (>50 equiv) of Et₂O to a benzene-*d*₆ solution of either **1** or **2** produced C–O cleavage products with no spectroscopic evidence for intermediates.

Cleavage of the C–O bond in diethyl ether was also accomplished with the more electron-rich, alkylated η^9, η^5 -bis(indenyl)zirconium sandwich, (η^9 -C₉H₅-1,3-(CHMe₂)₂)(η^5 -C₉H₅-1,3-(CHMe₂)₂)Zr (**5**).²³ Stirring **5** in neat diethyl ether for 36 h at 45 °C yielded the zirconocene ethoxy hydride (η^5 -C₉H₅-1,3-(CHMe₂)₂)Zr(OEt)H (**5**-(OEt)H) and the metallacycle **5**-(*c*-C₄H₈), arising from coupling of 2 equiv of ethylene (eq 3). A 2:1 ratio of **5**-(OEt)H to **5**-(*c*-C₄H₈) was consistently observed. Previous studies from our laboratory have demonstrated that the less sterically congested sandwich compound promotes more facile coupling of olefins and alkynes.¹² Indeed, addition of



(19) For an example of a crystallographically characterized base-free *ansa*-zirconocene alkyne complex, see: Lefebvre, C.; Baumann, W.; Tillack, A.; Kempe, R.; Görls, H.; Rosenthal, U. *Organometallics* **1996**, *15*, 3486.

(20) Fischer, R.; Walther, D.; Gebhardt, P.; Görls, H. *Organometallics* **2000**, *19*, 2532.

(21) Lee, H.; Hascall, T.; Desrosiers, P. J.; Parkin, G. *J. Am. Chem. Soc.* **1998**, *120*, 5830.

(22) Cohen, S. A.; Auburn, P. R.; Bercaw, J. E. *J. Am. Chem. Soc.* **1983**, *105*, 1136.

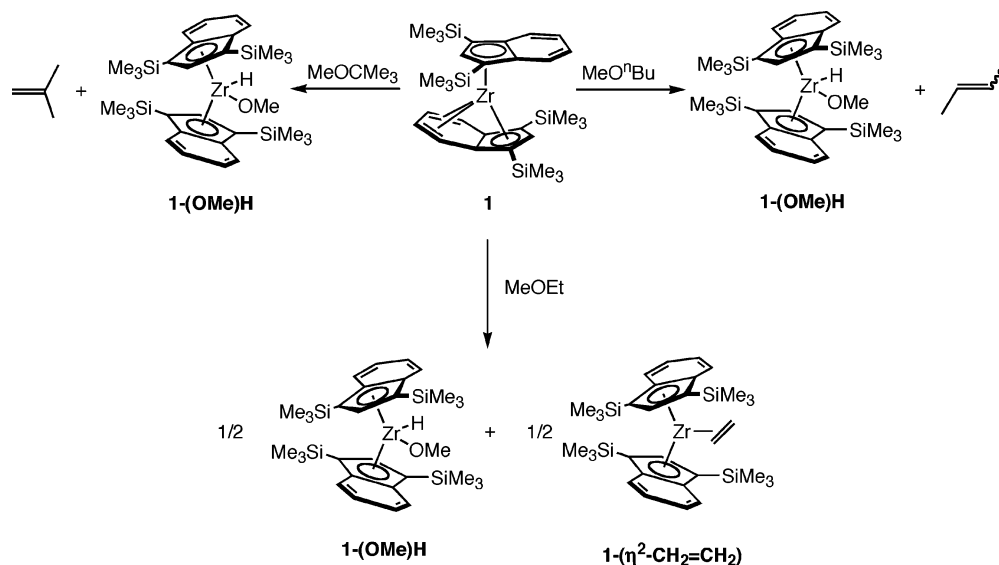


Figure 3. Products of methyl alkyl ether cleavage with **1**.

ethylene to **5** in benzene-*d*₆ yielded only **5-(*c*-C₄H₈)** independent of the amount of olefin employed. Qualitatively, the rates of diethyl ether cleavage with **1** and **2** were indistinguishable, whereas those with **5** was slower.

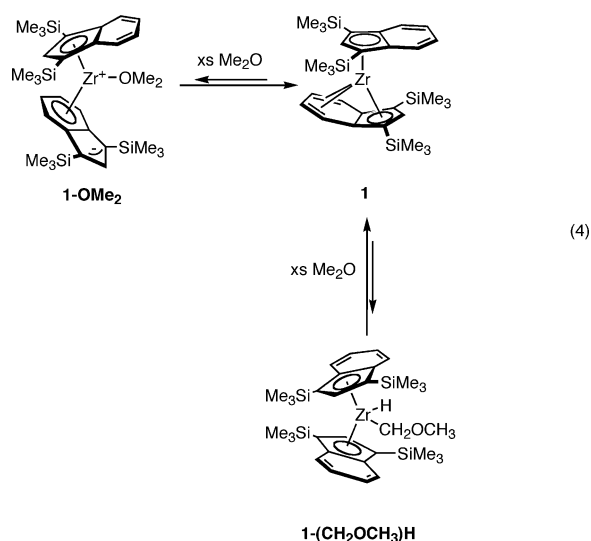
The observation of carbon–oxygen bond cleavage of diethyl ether to yield well-defined zirconocene products prompted further exploration into the scope of the reaction. The silylated sandwich, **1**, was used for the majority of subsequent studies due to its relative ease of synthesis and high symmetry. In certain instances, the chemistry of **5** was also examined due to its smaller indenyl substituents and more electron-rich zirconium center.²⁴

Methyl alkyl ethers, MeOR (R = Et, ⁿBu, ^tBu), were initially studied. Selective C–O bond cleavage of the ethers was observed when large excesses, either neat solution or 50 equiv in benzene-*d*₆, were stirred with **1**. In each case, the zirconocene methoxy hydride compound, (η^5 -C₉H₅-1,3-(SiMe₃)₂)₂Zr(OCH₃)H (**1-(OMe)H**), was observed along with a corresponding olefin byproduct (Figure 3).

For MeOEt, the olefin product of C–O cleavage is ethylene which is readily trapped by free sandwich compound to yield **1-(η^2 -CH₂=CH₂)**. In the case of methyl *n*-butyl ether cleavage, a thermodynamic mixture of free *cis*- and *trans*-2-butene was identified by ¹H NMR spectroscopy. Previous work from our laboratory has demonstrated that **1** isomerizes terminal olefins to internal olefins, most likely through zirconocene crotyl hydride intermediates.¹² Once the 2-butenes are formed, the olefins are sufficiently hindered such that coordination to zirconium is not observed. This trend also holds for MeOⁿBu (MTBE) cleavage, where 1 equiv of free isobutene was observed.

Treatment of **1** with dimethyl ether produced a different outcome. Monitoring the addition of 50 equiv of Me₂O to a benzene-*d*₆ solution of **1** by ¹H NMR spectroscopy revealed approximately 10% conversion to the η^6, η^5 -bis(indenyl)zirconium dimethyl ether adduct (**1-OMe₂**) after 15 min at 23 °C

(eq 4). The rest of the material was starting sandwich **1** and excess dimethyl ether.



Diagnostic resonances¹⁷ for η^6, η^5 -indenyly coordination were observed at 3.36 and 3.55 ppm assigned to a cyclopentadienyl hydrogen on the η^5 ring and a benzo hydrogen on the η^6 ligand, respectively. Over the course of minutes at 23 °C, a new C_s symmetric product identified as the zirconocene alkyl hydride, (η^5 -C₉H₅-1,3-(SiMe₃)₂)₂Zr(CH₂OCH₃)H (**1-(CH₂OCH₃)H**), was observed (eq 4). This compound arises from C–H activation of an ether methyl group and exhibits cyclopentadienyl and benzo hydrogens in the 6.50 to 7.50 ppm chemical shift region, indicative of common η^5, η^5 indenyl hapticity. Exposure of the product mixture to a vacuum resulted in the loss of dimethyl ether, from either dissociation or reductive elimination, and allowed isolation of the sandwich, **1**. Warming the reaction mixture to 85 °C for several days produced a complex mixture of products, the majority of which contained **1**, the corresponding zirconocene cyclometalated hydride and **1-(CH₂OCH₃)H**. Importantly, no C–O bond cleavage was observed under these conditions.

(23) The labeling scheme used in this paper is adapted from ref 12.

(24) Bradley, C. A.; Flores-Torres, S.; Lobkovsky, E.; Abruña, H. D.; Chirik, P. J. *Organometallics* **2004**, *23*, 5332.

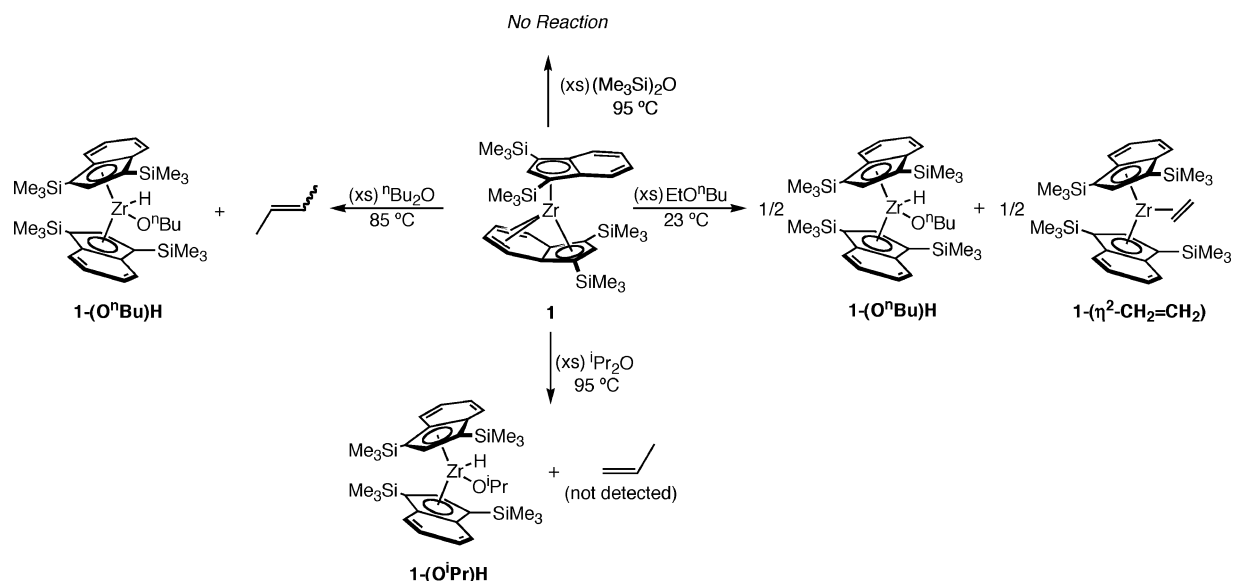
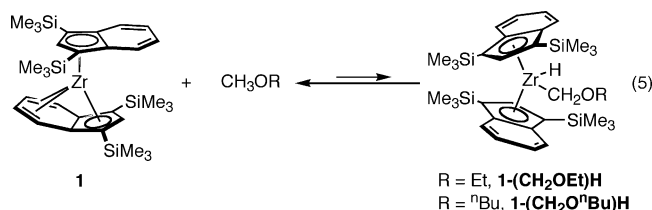


Figure 4. Products of longer chain dialkyl ether cleavage with **1**.

Observation of C–H activation with dimethyl ether prompted more careful monitoring of the addition of other methyl alkyl ethers to **1**. Addition of 10 equiv of methyl ethyl ether or 50 equiv of methyl *n*-butyl ether to **1** in benzene-*d*₆ allowed observation of small quantities (10–30%) of the corresponding zirconocene alkyl hydride compounds, (η^5 -C₉H₅-1,3-(SiMe₃)₂-Zr(CH₂OR)H (R = Et, **1**-(CH₂OEt)H; ⁿBu, **1**-(CH₂OⁿBu)H), over the course of minutes at 23 °C (eq 5).



For both zirconocene alkyl hydride compounds, diagnostic resonances upfield of 0 ppm were observed for the diastereotopic hydrogens on the carbon directly bound to the zirconium. No benzo or cyclopentadienyl peaks were present between 3 and 5 ppm that are indicative of η^6 indenyl coordination. Additional evidence for C–H activation was provided by degradation experiments. Treatment of **1**-(CH₂OEt)H or **1**-(CH₂OⁿBu)H with an excess of gaseous deuterium chloride afforded ROCH₂D and **1**-Cl₂. No ¹H NMR spectroscopic evidence for C–H activated products or η^6, η^5 -bis(indenyl)zirconium ether complexes was obtained upon treatment of **1** with a large excess of methyl *tert*-butyl or diethyl ether.

Carbon–oxygen bond cleavage in longer chain dialkyl ethers was also explored. Treatment of a benzene-*d*₆ solution of **1** with 20 equiv of ethyl *n*-butyl ether produced an equimolar mixture of (η^5 -C₉H₅-1,3-(SiMe₃)₂-Zr(OⁿBu)H (**1**-(OⁿBu)H) and **1**-(η^2 -CH₂=CH₂) over the course of 3 days at 23 °C (Figure 4). Thermolysis with di-*n*-butyl ether at 85 °C under similar conditions furnished **1**-(OⁿBu)H and a mixture of *cis*- and *trans*-2-butene. Likewise, heating a benzene-*d*₆ solution of **1** to 95 °C in the presence of 25 equiv of *i*Pr₂O yielded (η^5 -C₉H₅-1,3-(SiMe₃)₂-Zr(OⁱPr)H (**1**-(OⁱPr)H) after 5 days. The presumed olefin byproduct, propene, was not detected by ¹H NMR spectroscopy.

Table 2. Pseudo-First-Order Rate Constants Measured for Et₂O Cleavage with **1** at 45 °C^a

equiv of Et ₂ O	$k_{\text{obs}} \times 10^3 \text{ (s}^{-1}\text{)}$
10	1.1(2)
25	1.4(2)
50	2.2(3)
75	4.1(3)

^a Each experiment was conducted with a 0.03 M solution of **1** in benzene-*d*₆.

Attempts to cleave (Me₃Si)₂O were unsuccessful; heating **1** to 95 °C in the presence of a large excess of ether produced no Si–O cleavage products after 2 weeks.

To probe the mechanism of dialkyl ether cleavage, several kinetic and isotopic labeling experiments were performed. Rate constants for diethyl ether cleavage by **1** were measured at 45 °C in benzene-*d*₆ solution by ¹H NMR spectroscopy with Et₂O excesses ranging between 10 and 75 equiv. Under these conditions, clean pseudo-first-order processes were obtained (see Supporting Information). The observed rate constants from these experiments are reported in Table 2. The nonlinear, nearly sigmoidal dependence of the observed rate constant is most likely a result of competing pathways involving diethyl ether cleavage and coordination. One path is a productive mechanism involving initial C–H bond cleavage ultimately leading to C–O scission while the others are most likely due to ligand induced haptotropic rearrangement to form η^6, η^5 -bis(indenyl)zirconium mono- and bis(ether) complexes. Previous studies have shown that addition of 1 and 2 equiv of THF to **1** results in a similar outcome where both processes are dependent on the THF concentration.¹⁷

The kinetic isotope effect ($k_{\text{H}}/k_{\text{D}}$) for dialkyl ether cleavage was also measured for both **1** and **2**. Using Et₂O as a representative substrate, benzene-*d*₆ solutions of **1** or **2** were prepared with an equimolar mixture of diethyl ether and diethyl ether-*d*₁₀. A combination of ¹H and ²H NMR spectroscopy was used to confirm the formation of the expected products: **1**-(OEt)H, **1**-(OEt-*d*₅)D, **1**-(η^2 -CH₂=CH₂), and **1**-(η^2 -CD₂=CD₂). The kinetic isotope effects were measured by monitoring the C–O bond cleavage as a function of time by integration of the Zr–H resonance of **1**-(OEt)H versus the indenyl ring

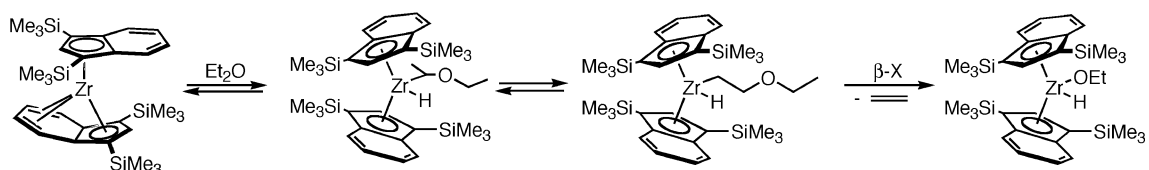
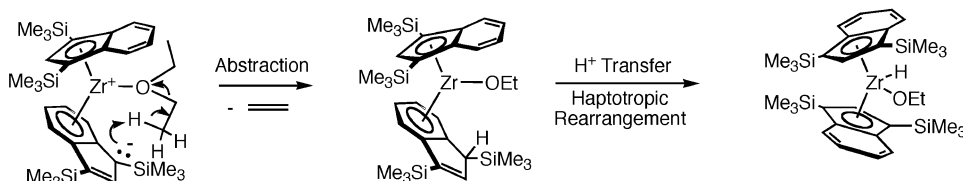
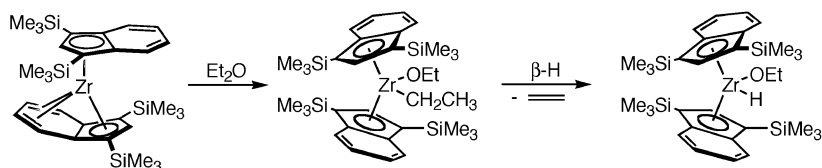
Path A: η^5, η^5 Intermediates**Path B:** η^6, η^5 Intermediates**Path C:** C–O Oxidative Addition

Figure 5. Mechanistic possibilities for dialkyl ether cleavage with η^9, η^5 -bis(indenyl)zirconium sandwich compounds.

protons for both isotopologs of the bis(indenyl)zirconium ethoxy hydride(deuteride) compounds. Resonances for the two isotopologs of the ethylene compounds could not be used as competing isotopic exchange with the $[\text{SiMe}_3]$ complicated the integration values. A similar control, whereby a benzene- d_6 solution of **1-(OEt)H** and **1-(OEt- d_5)D** was allowed to stand at 23 °C for several days, produced no isotopic exchange. From the average of four independent trials, a normal primary isotope effect ($k_{\text{H}}/k_{\text{D}}$) of 5.0(5) was measured at 23 °C. A statistically indistinguishable value of $k_{\text{H}}/k_{\text{D}}$ of 4.7(4) was determined for **2** from seven independent trials. These data clearly indicate that a C–H bond cleavage event precedes C–O bond scission either in or prior to the rate-determining step.

At this point, it is useful to consider possible mechanisms for dialkyl ether cleavage. Three general mechanistic proposals are presented in Figure 5 using diethyl ether as a representative substrate and **1** as the η^9, η^5 -bis(indenyl)zirconium sandwich. Path A involves C–H activation by **1**, through a transient η^5, η^5 -bis(indenyl)zirconium sandwich (not shown), to yield a zirconocene alkyl hydride complex. Subsequent β -alkoxide elimination^{25,26} liberates free ethylene which is trapped by unreacted **1** to yield the observed zirconocene ethoxy hydride product. C–H activation at the position adjacent to the oxygen is shown, though activation of other positions along the chain are also plausible. The second pathway involves η^6, η^5 -bis(indenyl)zirconium intermediates and must be considered as these species have been isolated from addition of THF or DME to **1**.¹⁷ In Path B, only one possibility involving η^6 haptomers is illustrated: γ -C–H activation promoted by the η^6 indenyl ligand followed by proton transfer and haptotropic rearrangement. Both

Wolczanski²⁷ and Parkin²⁸ have provided a precedent for γ -C–H activation in group 4 transition metal chemistry with titanium amide and zirconium oxo complexes, respectively. Other possibilities for C–H activation, especially those similar to Path A, leading to C–O scission are possible from η^6 indenyl intermediates, but only one is shown for convenience. The final mechanism, Path C, involves direct oxidative addition of the C–O bond to form an intermediate zirconocene alkoxy alkyl complex which then undergoes β -hydride elimination to form ethylene (trapped by **1**) and the observed zirconocene ethoxy hydride compound.

In an attempt to definitively exclude the possibility of Path C, the synthesis of a putative zirconocene alkoxy alkyl complex was targeted. Alkylation of **1-(OMe)Cl**, prepared from methyl vinyl ether addition to **1-(H)Cl**, with $^n\text{BuLi}$ yielded the zirconocene methoxy butyl compound (η^5 - C_9H_5 -1,3-(SiMe_3)₂-Zr(OMe) n Bu (**1-(OMe) n Bu**), the requisite intermediate arising from C–O oxidative addition from MeO^nBu cleavage. Heating a benzene- d_6 solution of **1-(OMe) n Bu** to 65 °C for 2 days produced no change in the ^1H NMR spectrum. Recall that cleavage of MeO^nBu occurred at 23 °C in a similar time frame, definitely excluding Path C as the mechanism of dialkyl ether cleavage. The selectivity of the MeOR cleavage reactions is also inconsistent with a direct C–O oxidative addition pathway. Selective formation of **1-(OMe)H** would not be expected for the series of ethers (Figure 3).

The feasibility of the C–H activation/ β -alkoxide elimination sequence found in Path A (and possibly in a variant of Path B) was probed by a series of olefin insertion studies.²⁹ The synthesis of a stable bis(indenyl)zirconium dihydride complex, (η^5 - C_9H_5 -

(25) Strazisar, S. A.; Wolczanski, P. T. *J. Am. Chem. Soc.* **2001**, *123*, 4728.

(26) For examples of β -chloride eliminations in group 4 metallocene chemistry, see: Stockland, R. A.; Foley, S. R.; Jordan, R. F. *J. Am. Chem. Soc.* **2003**, *125*, 796.

(27) Schaller, C. P.; Cummins, C. C.; Wolczanski, P. T. *J. Am. Chem. Soc.* **1996**, *118*, 591.

(28) Howard, W. A.; Waters, M.; Parkin, G. *J. Am. Chem. Soc.* **1993**, *115*, 4917.

(29) For synthesis of similar compounds in cyclopentadienyl-based chemistry, see: Buchwald, S. L.; Nielsen, R. B.; Dewan, J. C. *Organometallics* **1998**, *7*, 2324.

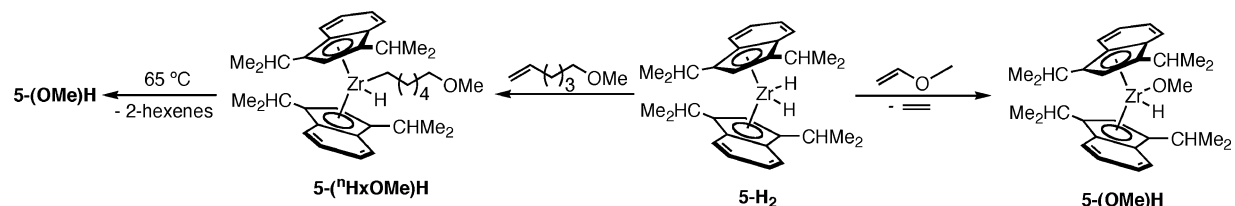


Figure 6. Evaluation of β -alkoxide elimination with 5-H_2 .

1,3-(CHMe₂)₂ZrH₂ (5-H_2), was accomplished by oxidative addition of H₂ to **5** at 23 °C.³⁰ Importantly, this procedure allows isolation of the dihydride where the benzo rings remain intact and do not undergo hydrogenation to the corresponding tetrahydroindenyl derivative. Ring hydrogenation was only observed with continued exposure to H₂ at 45 °C.

Addition of 1 equiv of methyl vinyl ether to a benzene-*d*₆ solution of 5-H_2 at 23 °C immediately yielded 5-(OMe)H and free ethylene (Figure 6). These products are a result of olefin insertion into the Zr–H bond followed by rapid β -OMe elimination; no resonances for the intermediate zirconocene alkyl hydride were detected by ¹H NMR spectroscopy. A similar experiment was also performed with 1-hexenyl methyl ether.³¹ Addition of 1 equiv of the alkoxy-substituted olefin to a benzene-*d*₆ solution of 5-H_2 at 23 °C yielded the zirconocene alkyl hydride complex $5\text{-(}^n\text{HxOMe)H}$ immediately upon mixing. No chain running was observed until the solution was heated to 65 °C, whereupon 5-(OMe)H and a mixture of 2-hexenes was observed. These observations demonstrate that β -hydrogen elimination from terminal zirconocene alkyls is possible³² and continues until irreversible β -alkoxide elimination occurs. An alternative pathway would involve alkane reductive elimination to yield **5** followed by methylene C–H activation and β -methoxide elimination.

Based on the experimental data, previous work with bis(indenyl)zirconium complexes and computational studies on C–O activation for related THF compounds (vide infra), Path A is the favored mechanism for dialkyl ether cleavage. Previously our laboratory has demonstrated that the η^9, η^5 -bis(indenyl)zirconium sandwich, **1**, promotes the C–H activation of *N,N*-dimethylaminopyridine (DMAP), demonstrating that such species are capable of C–H activation.¹¹ In addition, solution NMR¹² and computational^{13,16} studies demonstrate that dissociation of the η^9 indenyl ring to form a transient η^5, η^5 -bis(indenyl)zirconium sandwich is energetically feasible at 23 °C. Moreover, C–H activation of the methyl groups of several ethers to yield ($\eta^5\text{-C}_9\text{H}_5\text{-1,3-(SiMe}_3)_2\text{Zr(CH}_2\text{OR)H}$) complexes have been observed. These compounds are not on the reaction coordinate for C–O bond cleavage, as β -alkoxide elimination is not possible. Importantly, these compounds are models for the C–H activation products of the longer alkyl chain. NMR spectroscopy has clearly established η^5 indenyl ligand coordination in the ($\eta^5\text{-C}_9\text{H}_5\text{-1,3-(SiMe}_3)_2\text{Zr(CH}_2\text{OR)H}$) derivatives, suggesting that productive C–H activation ultimately leading to β -alkoxide elimination also proceeds through η^5, η^5 -bis(indenyl)zirconium haptomers.

Because certain donors such as THF and DME are known to induce haptotropic rearrangement to form isolable η^6, η^5 -bis(indenyl)zirconium ligand derivatives, pathways that include such haptomers must be considered. As mentioned previously, the observation of η^5, η^5 haptomers arising from C–H activation argues against the formation of such species. In addition, the alkyl-substituted sandwich, **5**, does not coordinate THF to form the η^6, η^5 -bis(indenyl)zirconium THF complex even in neat THF.¹⁷ Initial spectroscopic¹⁷ and subsequent computational studies¹⁶ demonstrate that a stronger metal- η^9 indenyl interaction in the ground state coupled with a weaker Zr–O bond in the product, arising from a more electron-rich metal center, decreases the propensity for ligand-induced haptotropic rearrangement. Because **5** is competent for diethyl ether cleavage at rates only slightly slower than **1** and **2**, it appears that η^6 -haptomers are not a prerequisite for C–O bond scission. The slower rate observed with **5** is most likely a ground state effect, where a stronger η^9 interaction increases the barrier to access the intermediate η^5, η^5 -bis(indenyl)zirconium species required for C–H activation. The observed “leveling” in the rate constants for diethyl ether cleavage with **1** suggests that at higher ether concentrations formation of an unproductive η^6, η^5 -bis(indenyl)zirconium ether compound competes with formation of a productive η^5, η^5 -bis(indenyl)zirconium intermediate that is competent for rate-determining C–H activation followed by fast β -alkoxide elimination.

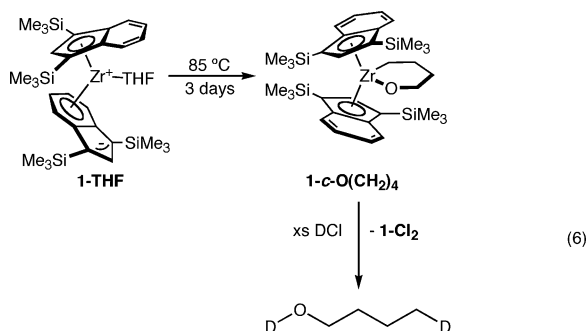
The observed selectivity in EtO^{*n*}Bu cleavage is also readily accommodated by mechanism A in Figure 5. Preferential C–H activation of the terminal methyl group of the ethyl chain leads to rapid, irreversible β -alkoxide elimination to form the observed products. The alternative pathway to form **1-(OEt)H** and 2-butenes would require either C–H activation of a more sterically hindered methylene position along the butyl chain or oxidative addition of the terminal methyl group followed by chain running. Both of these processes are expected to have higher barriers than those of the first pathway, and hence **1-(O^{*n*}Bu)H** and **1-($\eta^2\text{-CH}_2\text{=CH}_2$)** are formed exclusively.

Carbon–Oxygen Bond Cleavage of THF. Although η^5, η^5 -bis(indenyl)zirconium intermediates are favored for dialkyl ether cleavage, the possibility of C–O bond activation from isolable η^6, η^5 -bis(indenyl)zirconium ligand complexes was also explored. Thermolysis of a benzene-*d*₆ solution of ($\eta^6\text{-C}_9\text{H}_5\text{-1,3-(SiMe}_3)_2$)-($\eta^5\text{-C}_9\text{H}_5\text{-1,3-(SiMe}_3)_2\text{Zr(THF)}$) (**1-THF**) at 85 °C for several days resulted in clean and quantitative formation of the ring-opened product, ($\eta^5\text{-C}_9\text{H}_5\text{-1,3-(SiMe}_3)_2\text{Zr(cyclo-OCH}_2\text{(CH}_2)_2\text{-CH}_2$) (**1-c-O(CH}_2)_4**) (eq 6). The zirconocene alkoxy alkyl complex, **1-c-O(CH}_2)_4**, was characterized by multinuclear NMR spectroscopy, combustion analysis, and degradation experiments. Treatment with excess DCl produced **1-Cl}_2** and *O*-4-*d*₂-*n*-butanol, identified by ¹H and ²H NMR spectroscopy.

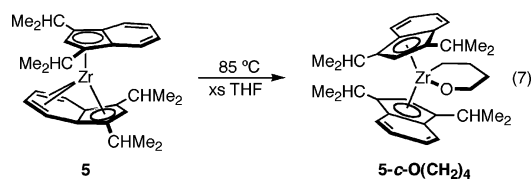
(30) Bradley, C. A.; Lobkovsky, E.; Keresztes, I.; Chirik, P. J. *J. Am. Chem. Soc.* **2006**, *128*, 6454.

(31) (a) Brown, H. C.; Lynch, G. J. *J. Org. Chem.* **1981**, *46*, 531. (b) Newcomb, M.; Filipkowski, M. A.; Johnson, C. C. *Tetrahedron Lett.* **1995**, *36*, 3643.

(32) Chirik, P. J.; Day, M. W.; Labinger, J. A.; Bercaw, J. E. *J. Am. Chem. Soc.* **1999**, *121*, 10308.



Carbon–oxygen bond cleavage in THF was also explored with zirconocene sandwich complexes that do not form isolable (or even observable) η^6, η^5 -bis(indenyl)zirconium-THF derivatives. Recall that the purely alkyl substituted **5** does not form any detectable quantity of **5-THF**, even in THF solution.¹⁷ Thermolysis of **5** at 85 °C in the presence of an excess of THF resulted in complete conversion to (η^5 -C₉H₅-1,3-(CHMe₂)₂)₂-Zr(*cyclo*-OCH₂(CH₂)₂CH₂) (**5-c-O(CH₂)₄**) after 3 days (eq 7).



The ring opened product, **5-c-O(CH₂)₄**, was characterized by multinuclear NMR spectroscopy (¹H, ¹³C), combustion analysis, and X-ray diffraction. Representations of the solid-state structure are presented in Figure 7. The overall molecular geometry of the compound is typical for a bent zirconocene derivative with two η^5 indenyl rings with a rotational angle of only 11.6(3)°, placing one benzo substituent over the metallocene wedge, similar to the geometry observed in a related crotyl hydride compound.¹² The six-membered metallacycle adopts a chairlike conformation with zirconium–carbon and zirconium–oxygen bond distances of 2.3007(11) and 1.9180(8) Å, similar to those in the related permethylated zirconocene complex, (η^5 -C₅Me₅)₂-Zr(*cyclo*-O(CH₂)₄), prepared by treatment of the zirconocene dichloride with BrMgCH₂(CH₂)₂CH₂OMgBr.³³

Mechanistic Studies for THF Cleavage. As with diethyl ether cleavage, kinetic studies were performed on the ring opening of THF with **1**. Experiments were performed at 85 °C with excesses of THF ranging between 10 and 75 equiv. The pseudo-first-order rate constants are presented in Table 3 and were determined from monitoring the conversion of **1-THF** to **1-c-O(CH₂)₄** by ¹H NMR spectroscopy as a function of time.

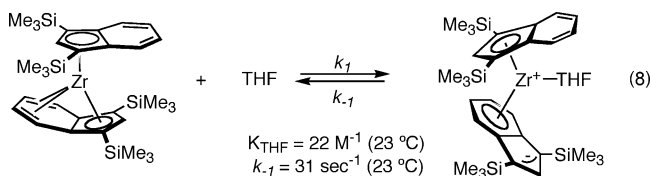
The data compiled in Table 3 clearly establish that the rate of C–O bond cleavage is independent of the THF concentration. We have previously measured both the equilibrium and rate constants for THF coordination to **1**.¹⁷ In benzene-*d*₆ at 23 °C, the equilibrium constant for the addition of THF to **1** is 22 M⁻¹,

Table 3. Observed Pseudo-First-Order Rate Constants for C–O Bond Cleavage in THF with **1** at 85 °C^a

equiv of THF	$k_{\text{obs}} \times 10^3$ (s ⁻¹)
10	1.8(1)
50	1.9(1)
75	1.8(1)

^a Each experiment conducted at 0.03 M **1** in benzene-*d*₆.

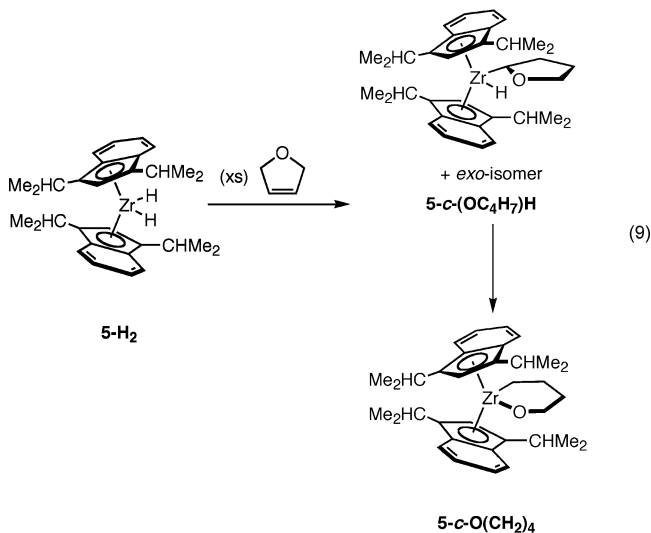
while the first-order rate constant for THF dissociation is 31 s⁻¹ (eq 8). Comparing the latter value to the rate constants



measured for THF cleavage demonstrates that THF dissociation to generate the η^9, η^5 -bis(indenyl)zirconium sandwich is fast and reversible relative to the C–O bond cleavage reaction.

Kinetic isotope effects for THF scission were also measured. Competition experiments were conducted, whereby benzene-*d*₆ solutions of **1** were heated to 92 °C with excesses of equimolar mixtures of THF and THF-*d*₈. The conversion was monitored as a function of time by integrating the ¹H NMR resonances of the indenyl ring protons relative to the metallo-cycle. This procedure yielded a value of $k_{\text{H}}/k_{\text{D}}$ of 3.5(3) at 92 °C as the average of five independent trials. The control experiment where **1-c-O(CD₂)₄** was heated to 92 °C for 12 h was conducted and produced no isotopic exchange into the [SiMe₃] substituents. As with diethyl ether cleavage, the observation of a normal, primary kinetic isotope effect establishes a C–H bond-breaking step along the reaction coordinate either in or before the rate-determining step.

The synthesis of potential intermediates from olefin insertion with the bis(indenyl)zirconium dihydride **5-H₂** was also explored. Treatment of **5-H₂** with excess (>25 equiv) 2,5-dihydrofuran at –78 °C followed by warming to ambient temperature yielded the zirconocene alkyl hydride complex **5-(c-OC₄H₇)H**, where the zirconium has migrated to the carbon α to the oxygen atom (eq 9). The ¹H NMR spectrum of **5-(c-**



OC₄H₇)H exhibits the number of resonances consistent with a near equimolar mixture of endo and exo isomers, where the endo isomer is defined as the one in which the oxygen atom of the ring is coordinated in the central position of the zirconocene wedge. Catalytic isomerization of the bulk 2,5-dihydrofuran to the 3,4 isomer occurred immediately upon addition to **5-H₂**.

(33) Mashima, K.; Yamakawa, M.; Takaya, H. *J. Chem. Soc., Dalton Trans.* **1991**, 2851.

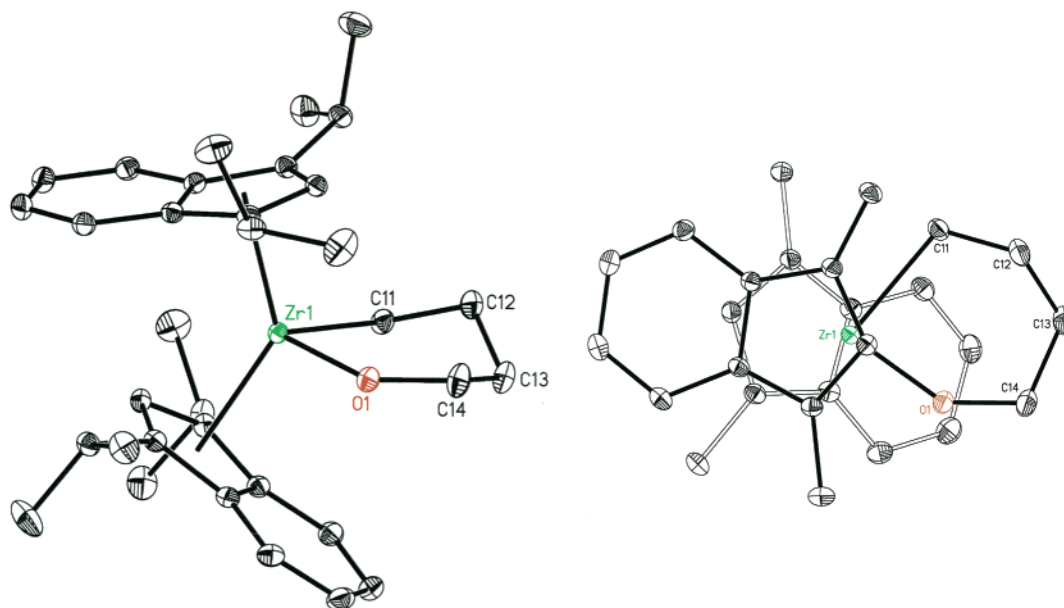
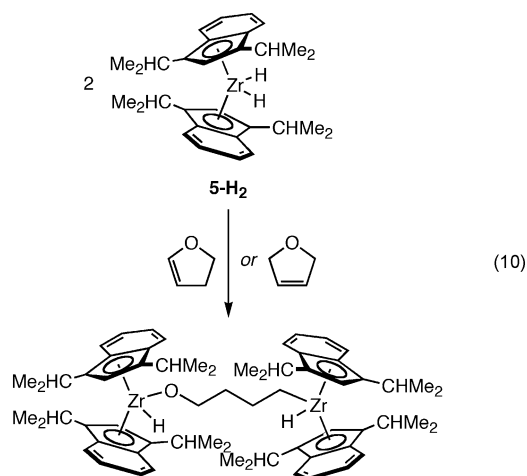


Figure 7. Molecular structure of **5-c-O(CH₂)₄** at 30% probability ellipsoids (left). Hydrogen atoms omitted for clarity. Top view of the molecule with hydrogens and isopropyl methyl substituents removed for clarity (right).

Confirmation of the position of the zirconium atom on the ring was accomplished by treatment with DCl, which yielded **5-Cl₂** with deuterium exclusively in the position α to the oxygen.

Over the course of hours at 23 °C in a benzene-*d*₆ solution, **5-c-OC₄H₇H** gradually converts to the product of THF scission **5-c-O(CH₂)₄**. Unfortunately attempts to gain more mechanistic insight by treating **5-D₂** with 2,5-dihydrofuran have been unsuccessful as the isotopic labels are rapidly washed into the excess olefin required for synthesis. Despite this limitation, these results demonstrate that an observable C–H activated product leads to C–O bond cleavage under mild conditions.

Failure to add an excess of either 3,4- or 2,5-dihydrofuran to **5-H₂** produced a different outcome. Under these conditions, bimetallic insertion/ring opening to the bridging alkoxy alkyl zirconocene hydride complex was observed (eq 10). Treatment

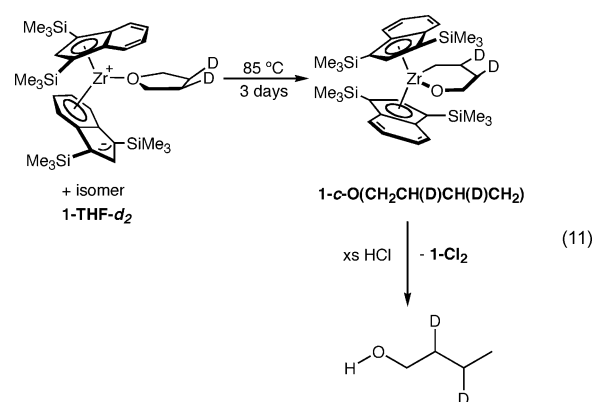


of this compound with 1 atm of dihydrogen at 45 °C yielded the bis(tetrahydroindenyl)zirconocene dihydride, **5-THI-H₂**,³⁰ and the alkoxy hydride, **5-(OⁿBu)H**.

The C–O bond cleavage of 3,4-*d*₂-THF with **1** was also explored. This substrate was prepared in a straightforward manner by D₂ addition to 2,5-dihydrofuran using Crabtree's

catalyst, [(COD)Ir(PPh₃)(py)]PF₆ (COD = 1,5-cyclooctadiene, py = pyridine). Using this procedure, less than 5% deuterium incorporation into the positions adjacent to the oxygen was detected by ²H NMR spectroscopy. Other catalysts such as (Ph₃P)₃RhCl produced higher levels of isotopic scrambling.

Addition of 3,4-*d*₂-THF to a benzene-*d*₆ solution of **1** afforded the η^6, η^5 -bis(indenyl)zirconium-THF-*d*₂ complex, **1-THF-*d*₂**. Two isomers (one with the deuterium atoms syn to the η^6 ring, the other with the deuteria anti) are most likely formed; however they are not resolved by ¹H NMR spectroscopy in part due to the rapid dissociation and recoordination of the THF-*d*₂ ligand.¹⁷ Thermolysis of **1-THF-*d*₂** at 85 °C for 3 days resulted in ring opening to yield the oxozirconacycle without scrambling of the deuterium positions as judged by ²H and ¹³C NMR spectroscopy (eq 11). The assignment of the ¹³C NMR spectrum (Figure 8)



was accomplished by comparison of chemical shifts to known bis(indenyl)zirconium compounds as well as with a *g*-HSQC experiment. The appearance of two triplets in the {¹H}¹³C experiment for the carbons labeled “2” and “3” is consistent with selective deuterium incorporation. Degradation of the labeled ring opened product with excess HCl was consistent with this observation yielding **1-Cl₂** and 2,3-*d*₂-butan-1-ol exclusively (eq 11).

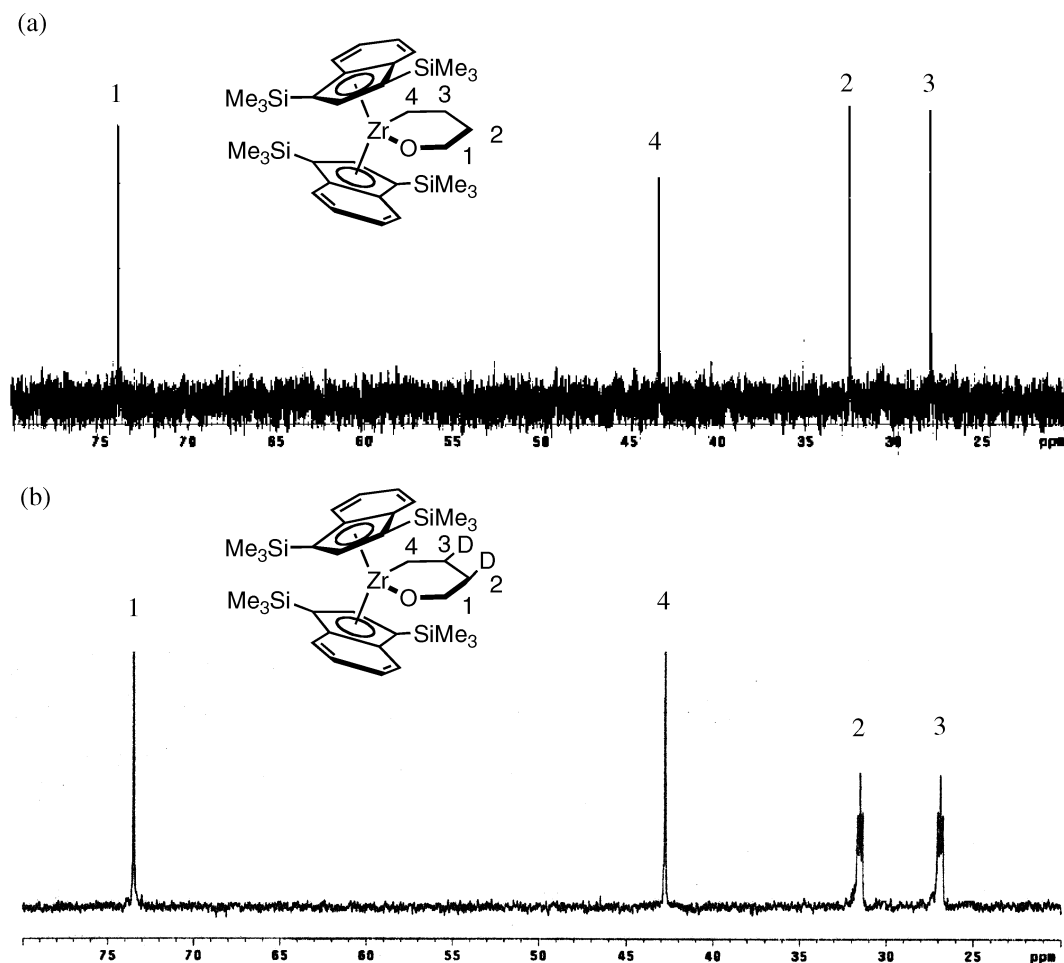


Figure 8. Partial $\{^1\text{H}\}^{13}\text{C}$ NMR spectra of (a) $1\text{-c-O}(\text{CH}_2)_4$ and (b) $1\text{-c-O}(\text{CH}_2\text{CH}(\text{D})\text{CH}(\text{D})\text{CH}_2)$ in benzene- d_6 .

The results of the isotopic labeling experiment with 3,4-THF- d_2 establish that chain running via reversible β -hydrogen elimination to the 3 or 4 position of the THF ring, while plausible from the model studies, is not a prerequisite for C–O bond cleavage. If this were the case, deuterium scrambling into the 1 and 4 positions (Figure 8) would be expected.

Computational Studies. The mechanism of both C–H and C–O bond activation of THF by bis(indenyl)zirconium sandwich complexes was also investigated with DFT calculations³⁴ using model complexes, whereby the 1,3-disubstituted indenyl ligands were replaced with the parent indenyl anion, $[\text{C}_9\text{H}_7]^-$. The possibility of both bond activation reactions from the η^6, η^5 -bis(indenyl)zirconium THF complex, $(\eta^6\text{-C}_9\text{H}_7)(\eta^5\text{-C}_9\text{H}_7)\text{Zr}(\text{THF})$ (**A**) was initially computed. The free energy profile³⁵ for these processes is presented in Figure 9.

The mechanism for C–H bond breaking from **A** (left side, Figure 9) follows a single-step pathway. The reaction profile corresponds to the oxidative addition of one C–H bond to the zirconium, forming the zirconocene alkyl hydride complex, **B**, where the η^6, η^5 hapticity of the indenyl rings is maintained. In the transition state, **TS_{AB}**, the scission of the C–H bond is just started, while the formation of the Zr–H bond is nearly complete with a Zr–H distance of 1.87 Å, only slightly longer than the value of 1.82 Å found in the final product **B**. The Wiberg indices

(WI)³⁶ also support this trend as the Zr–H has a value of 0.481 in **TS_{AB}** and 0.776 in **B**; the C–H bond has a value of 0.383 in **TS_{AB}** and 0.037 in **B**. The Zr–O bond is maintained throughout the course of the reaction as evidenced by the bond distances: $d_{\text{Zr-O}} = 2.32, 2.34,$ and 2.30 Å, in **A**, **TS_{AB}**, and **B**, respectively. This interaction becomes progressively stronger along the reaction coordinate ($\text{WI}_{\text{Zr-O}} = 0.239, 0.263,$ and 0.285 , by the same order). Perhaps most significantly, C–H activation from **A** is endergonic with $\Delta G = 8.0$ kcal/mol and a rather high activation energy of $\Delta G^\ddagger = 26.7$ kcal/mol.

The C–O bond breaking pathway from **A** also proceeds by a single-step process. In this case, the product is the zirconacycle (**C**) with η^6 and η^5 bound indenyl ligands. In this case, a dissociative mechanism is clearly operative as the new Zr–C bond has not started to form in the transition state (**TS_{AC}**) as $d_{\text{Zr-C}} = 3.44$ Å. Importantly, C–O bond breaking in THF is far advanced with an elongated bond length of 2.02 Å and weaker WI ($\text{WI}_{\text{C-O}} = 0.355$) than those of the reactant ($d_{\text{C-O}} = 1.47$ Å, $\text{WI}_{\text{C-O}} = 0.826$). Although the reaction is computed to be significantly exergonic, $\Delta G = -34.9$ kcal/mol, it involves a high activation barrier of $\Delta G^\ddagger = 22.1$ kcal/mol.

The values obtained for both C–H and C–O bond cleavage from **A** as well as the experimental results prompted an

(34) Parr, R. G.; Yang, W. *Density Functional Theory of Atoms and Molecules*; Oxford University Press: New York, 1989.

(35) All ΔG values were calculated at 298.15 K.

(36) (a) Wiberg, K. B. *Tetrahedron* **1968**, *24*, 1083. (b) Wiberg indices are electronic parameters related to the electron density in between atoms. They can be obtained from a Natural Population Analysis and provide an indication of the bond strength.

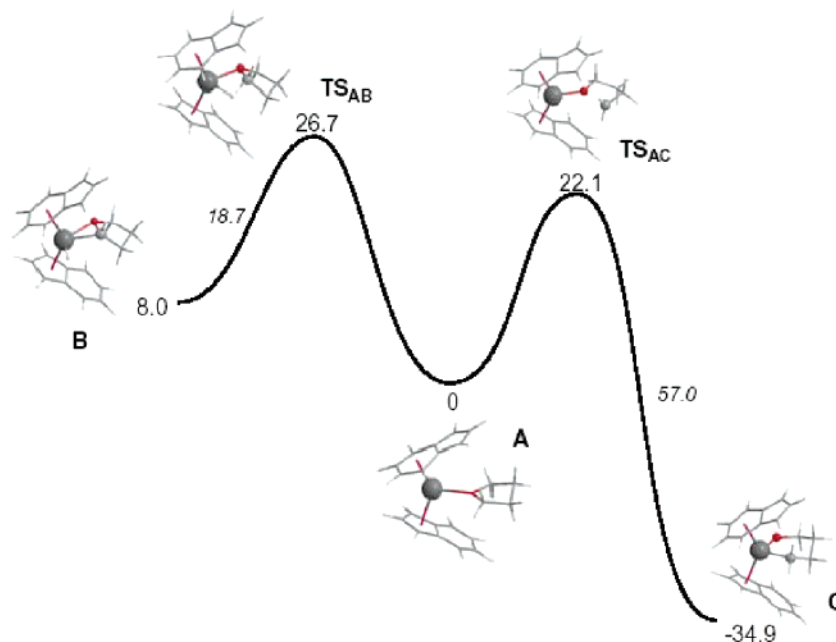


Figure 9. Free energy profile for the mechanism of C–H (left) and C–O (right) bond activation, starting from $(\eta^6\text{-C}_9\text{H}_7)(\eta^5\text{-C}_9\text{H}_7)\text{Zr}(\text{THF})$ (**A**). The minima and the transition states were optimized (B3LYP/VDZP), and the obtained structures are presented. The free energies (kcal mol^{-1}) are relative to **A**, and the values in italics represent energy barriers. The most relevant atoms in each step are highlighted.

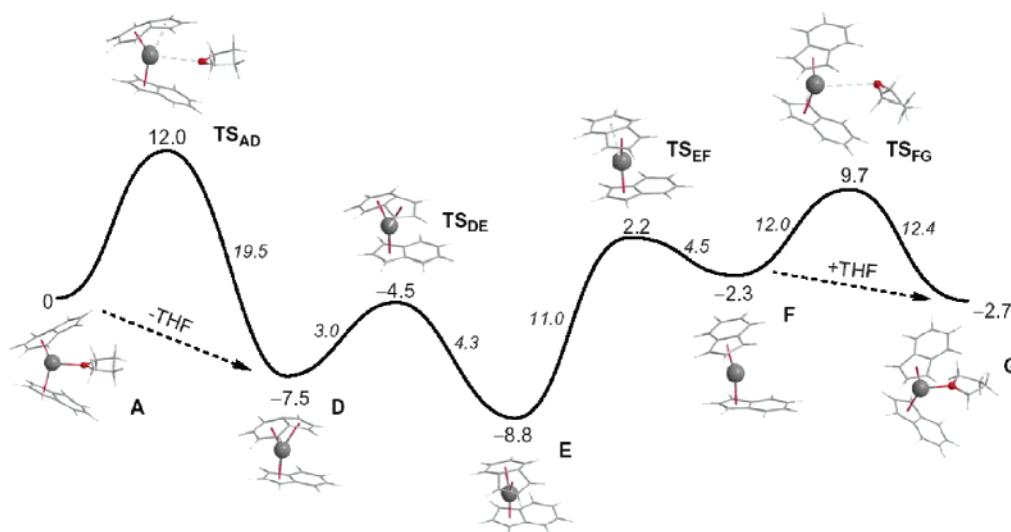


Figure 10. Free energy profile for the conversion of $(\eta^6\text{-C}_9\text{H}_7)(\eta^5\text{-C}_9\text{H}_7)\text{Zr}(\text{THF})$ (**A**) into $(\eta^5\text{-C}_9\text{H}_7)_2\text{Zr}(\text{THF})$ (**G**) by a dissociative mechanism. The minima and the transition states were optimized (B3LYP/VDZP), and the obtained structures are presented. The free energies (kcal mol^{-1}) are relative to **A**, and the values in italics represent energy barriers. The most relevant atoms in each step are highlighted.

investigation into alternative mechanistic possibilities. In these cases, the starting zirconium compound is the η^5, η^5 -haptomer of **A**, namely $(\eta^5\text{-C}_9\text{H}_7)_2\text{Zr}(\text{THF})$ (**G**). Therefore, the reaction of converting **A** to **G** was initially studied (Figure 10). There are two likely possibilities for this transformation. One is intramolecular with a direct shift of the hapticity of the η^6 indenyl to η^5 . The other possibility is dissociative, involving initial loss of THF to generate the η^9, η^5 -bis(indenyl)zirconium sandwich, $(\eta^9\text{-C}_9\text{H}_7)(\eta^5\text{-C}_9\text{H}_7)\text{Zr}$ (**E**), whereby readdition of THF yields $(\eta^5\text{-C}_9\text{H}_7)_2\text{Zr}(\text{THF})$ (**G**).

The dissociative conversion of **A** to **G** occurs in four discrete steps. The first two convert the η^6, η^5 complex, **A**, into the η^9, η^5 bis(indenyl)zirconium sandwich, $(\eta^9\text{-C}_9\text{H}_7)(\eta^5\text{-C}_9\text{H}_7)\text{Zr}$ (**E**). The first step is THF loss from **A** to produce $(\eta^9\text{-C}_9\text{H}_7)(\eta^5\text{-C}_9\text{H}_7)\text{Zr}$ (**D**), where the indenyl rings adopt an anti conformation.

Rotation of the indenyl ligands yields the gauche conformer, **E**, which converts to gauche $(\eta^5\text{-C}_9\text{H}_7)_2\text{Zr}$ (**F**) by benzo dissociation. Finally, **F** coordinates THF through a transition state (**TS_{FG}**) with the two molecules loosely bound ($d_{\text{Zr-O}} = 4.07 \text{ \AA}$). The overall activation free energy for this entire four-step process is 12.0 kcal/mol, well below the value computed (22.8 kcal/mol) for the intramolecular η^9 to η^5 shift¹³ and much lower than those computed for C–H and C–O activation from **A** (Figure 9).

The DFT computed free energy profile for THF cleavage from the η^5, η^5 -bis(indenyl)zirconocene THF adduct, **G**, is presented in Figure 11. The left side of the figure corresponds to direct C–O bond cleavage in the reactant, **G**, yielding the metallacycle $(\eta^5\text{-C}_9\text{H}_7)_2\text{Zr}(\text{O-}c\text{-(CH}_2)_4$) (**H**) in a single step. Similar to the mechanism from **A**, C–O bond cleavage is well advanced in

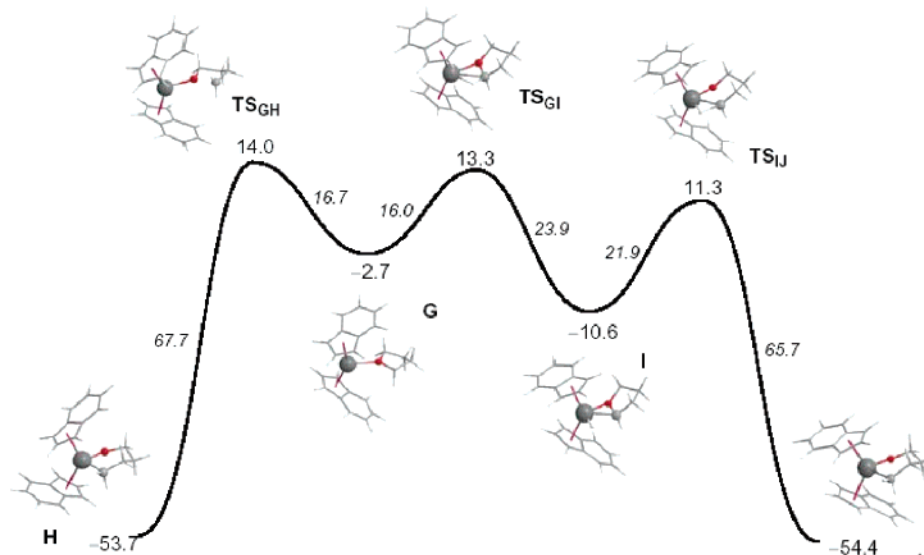


Figure 11. Free energy profile for the mechanism of C–H bond activation (right, two steps) and direct C–O bond breaking (left, one step), starting from $(\eta^5\text{-C}_9\text{H}_7)_2\text{Zr}(\text{THF})$ (**G**). The minima and the transition states were optimized (B3LYP/VDZP), and the obtained structures are presented. The free energies (kcal mol⁻¹) are relative to $(\eta^6\text{-C}_9\text{H}_7)(\eta^5\text{-C}_9\text{H}_7)\text{Zr}$ (**A**), and the values in italics represent energy barriers. The most relevant atoms in each step are highlighted.

the transition state ($d_{\text{C-O}} = 1.91 \text{ \AA}$, $\text{WI}_{\text{C-O}} = 0.422$). This process (**G** to **H**) is thermodynamically favorable with $\Delta G = -51.0 \text{ kcal/mol}$ and has an accessible activation free energy of $\Delta G^\ddagger = 14.0 \text{ kcal/mol}$.³⁷

The right side of Figure 11 corresponds to a two-step pathway involving initial C–H activation to yield an intermediate η^5, η^5 -bis(indenyl)zirconium alkyl hydride complex (**I**) that undergoes subsequent C–O bond cleavage to yield the final metallacycle product, **J**. The difference between **H** and **J** is simply the rotational conformation of the two indenyl ligands, and these rotamers are expected to interconvert readily in solution.^{12,13} The first step in the path leading from **G** to **J** is analogous to the corresponding C–H activation step from the η^6, η^5 -haptomer, **A** (Figure 9, left). In the transition state (**TS_{GI}**), the Zr–H bond is practically formed ($d_{\text{Zr-H}} = 1.89 \text{ \AA}$, $\text{WI}_{\text{Zr-H}} = 0.418$), and the C–H bond is still considerable ($d_{\text{C-H}} = 1.41 \text{ \AA}$, $\text{WI}_{\text{C-H}} = 0.466$). The conversion of **I** to **J** is concerted, and thus the C–O bond is weakened in the transition state (**TS_{IJ}**) with $d_{\text{C-O}} = 2.19 \text{ \AA}$ and $\text{WI}_{\text{C-O}} = 0.280$ as compared to **I** ($d_{\text{C-O}} = 1.49 \text{ \AA}$, $\text{WI}_{\text{C-O}} = 0.805$). The incipient C–H bond is nearly formed in **TS_{IJ}** ($d_{\text{C-H}} = 1.93 \text{ \AA}$, $\text{WI}_{\text{C-O}} = 0.231$), and both the carbon and oxygen atoms remain coordinated throughout the conversion from **I** to **J** ($d_{\text{Zr-O}} = 1.95\text{--}2.33 \text{ \AA}$, $d_{\text{Zr-C}} = 2.12\text{--}2.31 \text{ \AA}$). The transformation of **G** to **J** is thermodynamically favored with $\Delta G = -51.7 \text{ kcal/mol}$, and both steps have low activation free energies ($\Delta G^\ddagger = 13.3$ and 11.3 kcal/mol , respectively). Pathways involving C–H activation α to the oxygen were most favorable while those relying on activation of the β C–H bond were found to be much higher in free energy.

The computational studies demonstrate that the most favorable pathway for C–O bond cleavage in THF from **A** follows a multistep mechanism involving conversion of the η^6, η^5 -bis(indenyl)zirconium THF compound into the η^5, η^5 -haptomer followed by C–H activation and finally C–O bond breaking. The rate-determining step for the entire transformation is the C–H activation step (**G** \rightarrow **I**, $\Delta G^\ddagger = 13.3 \text{ kcal/mol}$) and is consistent with the experimentally observed normal, primary

kinetic isotope effect of 3.5(3) at 92 °C for THF versus THF-*d*₈ cleavage. Moreover, the initial dissociation of THF from the η^6, η^5 -bis(indenyl)zirconium THF compound to form the sandwich is followed by recoordination to yield the η^5, η^5 -haptomer prior to the rate-determining step and produces the overall zero-order dependence on THF concentration. C–H bond cleavage from the position adjacent to the oxygen without rearrangement to the β -position is also in agreement with the cleavage of 3,4-*d*₂-THF.

It should be noted that previous computational studies¹³ have identified the spin triplet form of $(\eta^5\text{-C}_9\text{H}_7)_2\text{Zr}(\text{THF})$ as being more stable by 2.8 kcal/mol than the singlet complex, **G**. Numerous attempts were made to find a plausible mechanism on the triplet spin surface, but all cases studied involved conversion to the singlet species, **G**, through the known¹³ crossing point, 3.2 kcal/mol above the triplet state itself. It should be pointed out that the computational studies were conducted on model compounds that lacked the sterically demanding 1,3-substituents, and these are known to attenuate the singlet–triplet gaps.¹⁶

Concluding Remarks

This study has demonstrated that η^9, η^5 -bis(indenyl)zirconium sandwich complexes are effective for C–O bond cleavage in dialkyl and cyclic ethers under mild conditions in solution to yield well-defined organic and organometallic products. Preparation of model compounds, in combination with kinetic, isotopic labeling, and computational studies, has established that the C–O activation reaction involves initial conversion of the η^9, η^5 -bis(indenyl)zirconium sandwich to reducing η^5, η^5 intermediates that promote C–H activation. In the dialkyl ether examples, subsequent β -alkoxide elimination generates the observed products. For isolable η^6, η^5 -bis(indenyl)zirconium THF compounds, dissociation of the oxygen donor followed by haptotropic rearrangement yields the active species for rate-determining C–H activation followed by C–O bond cleavage. In these reactions, isotopic labeling studies have eliminated competitive chain running during the course of THF opening.

(37) All energies are relative to the initial reactant, **A**.

These studies highlight the potential of isolable η^0, η^5 -bis-(indenyl)zirconium sandwich compounds to mediate formal two-electron reduction chemistry by access to η^5, η^5 -intermediates generated by facile benzo ring dissociation.

Experimental Section³⁸

Diethyl Ether Cleavage with 1. A 25 mL round bottomed flask was charged with 250 mg (0.41 mmol) of **1** and approximately 10 mL of diethyl ether. The reaction mixture was stirred at ambient temperature for 3 days. The solvent was removed in vacuo, and the resulting red foam was extracted into pentane. Analysis of the products by NMR spectroscopy revealed formation of a near equimolar mixture of **1-(η^2 -CH₂=CH₂)** and **1-(OEt)H**. Analytically pure **1-(η^2 -CH₂=CH₂)** can be isolated by successive recrystallizations (typically two) from pentane at -35 °C. However, attempts to obtain **1-(OEt)H** free from **1-(η^2 -CH₂=CH₂)** have been unsuccessful.

Characterization of (η^5 -C₉H₅-1,3-(SiMe₃)₂Zr(η^2 -C₂H₄)) 1-(η^2 -CH₂=CH₂). Anal. Calcd for C₃₂H₅₀Si₄Zr: C, 60.21; H, 7.90. Found: C, 59.89; H, 7.89. ¹H NMR (benzene-*d*₆): δ = 0.12 (s, 36H, SiMe₃), 0.87 (br s, 4H, C₂H₄), 6.67 (s, 2H, Cp), 7.07 (m, 4H, Benzo), 7.65 (m, 4H, Benzo). ¹³C NMR (benzene-*d*₆): δ = 1.34 (SiMe₃), 94.64 (C₂H₄), 110.03, 124.97, 125.26, 127.01, 136.27 (Cp/Benzo).

Characterization of (η^5 -C₉H₅-1,3-(SiMe₃)₂Zr(OCH₂CH₃)H) 1-(OEt)H. ¹H NMR (benzene-*d*₆): δ = 0.46 (s, 18H, SiMe₃), 0.49 (s, 18H, SiMe₃), 0.78 (t, 6 Hz, 3H, OCH₂CH₃), 3.37 (q, 6 Hz, 2H, OCH₂-CH₃), 5.16 (s, 2H, Cp), 5.23 (s, 1H, Zr-H), 6.74 (t, 8 Hz, 2H, Benzo), 6.81 (m, 2H, Benzo), 7.32 (d, 11 Hz, 2H, Benzo), 7.53 (d, 11 Hz, 2H, Benzo). ¹³C NMR (benzene-*d*₆): δ = 1.76, 1.86 (SiMe₃), 23.06 (OCH₂CH₃), 67.29 (OCH₂CH₃), 108.72, 123.46, 124.11, 124.93, 125.09, 125.25, 128.70, 133.83 (Cp/Benzo). One Cp/Benzo resonance not located.

General Kinetics Procedure. A flame-dried J. Young NMR tube was charged with 300 μ L of a 0.05 M benzene-*d*₆ stock solution of **1**

and 100 μ L of a 0.031 M benzene-*d*₆ solution containing sublimed ferrocene. The appropriate amount (typically 5–25 μ L) of dialkyl ether was then added by a microliter syringe, and benzene-*d*₆ was added to bring the total volume to 0.5 mL. The tube was then quickly shaken and frozen in liquid nitrogen. The tube was then transferred to a preheated NMR probe at the appropriate temperature (45 or 85 °C), and the disappearance of starting material and the appearance of product were measured in an arrayed ¹H NMR experiment. Typically the time interval between data collection was 1–5 min depending upon the reaction rate. Spectra were integrated versus the ferrocene standard. Three runs at each dialkyl ether concentration were performed.

Typical Procedure for Kinetic Isotope Effect Determination. A flame-dried J. Young NMR tube was charged with 300 μ L of a 0.04 M benzene-*d*₆ stock solution of **1** and 100 μ L of a 0.031 M benzene-*d*₆ solution containing sublimed ferrocene. 25 μ L (>25 equiv) of an equimolar solution of THF/THF-*d*₈ or diethyl ether/diethyl ether-*d*₁₀ was added to the tube. Dialkyl ether cleavage was then performed under typical conditions. The solvent was removed in vacuo on a vacuum line, and the samples were redissolved in 0.5 mL of benzene-*d*₆. Integration of the ¹H NMR resonances of the resulting cleavage products relative to ferrocene provided the kinetic isotope effects for the reactions.

Acknowledgment. We thank the National Science Foundation (CAREER Award to P.J.C. and predoctoral fellowship to C.A.B.) for financial support. P.J.C. also acknowledges the Research Corporation for a Cottrell Scholarship and the Packard Foundation for a fellowship in science and engineering.

Supporting Information Available: Additional experimental procedures, computational details, and spectral characterization. Crystallographic data for **1-(η^2 -CH₂=CH₂)** and **5-*c*-O(CH₂)₄** and all atomic coordinates for optimized species. This material is available free of charge via the Internet at <http://pubs.acs.org>.

(38) General considerations and additional experimental procedures are reported in the Supporting Information.

JA065456G